Paper:
Di Fraia, S., Massarotti, N., Mauro, A. & Nithiarasu, P. (2017). Heat and fluid flow in electro-osmotically driven systems. *Energy Procedia, 126*, 91-98.
http://dx.doi.org/10.1016/j.egypro.2017.08.069

Available online at www.sciencedirect.com

ScienceDirect

Energy Procedia 126 (201709) 91–98

Energy Procedia

www.elsevier.com/locate/procedia

72nd Conference of the Italian Thermal Machines Engineering Association, ATI2017, 6–8 September 2017, Lecce, Italy

Heat and fluid flow in electro-osmotically driven systems

Simona Di Fraia[a,*], Nicola Massarotti[a], Alessandro Mauro[a,b], Perumal Nithiarasu[c]

[a] *Dipartimento di Ingegneria, Università degli Studi di Napoli Parthenope, Isola C4, Centro Direzionale di Napoli, 80143 Napoli, Italy*
[b] *Università Telematica Pegaso, Piazza Trieste e Trento n.48, 80132 Napoli, Italy*
[c] *Biomedical Engineering and Rheology Group, Zienkiewicz Centre for Computational Engineering, Swansea University, Swansea SA2 8PP, United-Kingdom*

Abstract

A numerical investigation of heat and fluid flow in electro-osmotically driven systems is presented, by considering plain channels and channels packed with charged solid particles. The results show that the introduction of charged solid particles affects the internal potential distribution, fluid flow and temperature distribution in the channel. Under the analysed conditions, the effect on heat transfer is confined to the centre of the channel. This topic needs to be further investigated since it is of interest in practical applications.

Peer-review under responsibility of the scientific committee of the 72nd Conference of the Italian Thermal Machines Engineering Association

Keywords: Numerical modelling; CBS; Flow obstructions; Joule heating.

1. Introduction

Electro-osmotically driven flow systems are used for many applications in the field of biology and engineering, such as pumping, cooling, mixing and separation processes, and recently also for dehumidification and regeneration of desiccant structures [1]. In all these applications, the effect of heat transfer and Joule heating needs to be taken into account [2]. As an example, the analysis of heat transfer due to electro-osmotic flow can be useful in heat-dose sensitivity tests, needed to perform appropriately electromagnetic hyperthermia for the treatment of cancers and tumors [3].

The operation of electro-osmotically driven flow systems depends on the interaction between a solid surface and an electrolytic solution. In fact, a solid surface in contact with an electrolyte becomes spontaneously charged, usually negatively. The positive ions of the solution are then attracted and form a high concentration region close to the charged surface. This high concentration region is called Electric Double Layer (EDL) [4]. Under the application of an external electric field the ions accumulated in the EDL tend to restore the electro-neutrality of the system, moving

* Corresponding author. Tel.: +39-081-547-6709.
E-mail address: simona.difraia@uniparthenope.it

1876-6102 © 2017 The Authors. Published by Elsevier Ltd.
Peer-review under responsibility of the scientific committee of the 72nd Conference of the Italian Thermal Machines Engineering Association
10.1016/j.egypro.2017.08.069

towards the negative electrode. As a result, the nearby ions are also dragged and Electro-Osmotic Flow (EOF) is produced. As the distance from the charged surface increases, the ionic concentration reduces and, as a consequence, EDL effect decreases. For this reason, EOF driven systems are effective at micro- and nano-scale. In plain channels, only the walls play a role as charged surfaces, while when solid particles are introduced inside channels, their charged boundaries can also be taken into account. As a consequence, EOF can potentially be enhanced.

As Joule heating increases, the fluid temperature was found to increase [5, 6]. The Joule heating effect was observed to grow with the capillary size [7, 8], the strength of the applied electrical field [7, 9] and the solution concentration [7, 10]. Several authors studied the Joule heating effect by considering temperature dependence to determine the thermo-physical properties of the system [7, 10, 11, 5], while others neglected this dependence [12, 8]. In fact, it was demonstrated that fluid properties can be assumed to be constant when EDL becomes sufficiently thin [13].

Tang et al. [7] proposed a numerical analysis of Joule heating effect on the electroosmotic flow and mass species transport. Temperature distribution in the liquid presented a parabolic shape, with the highest temperature occurring at the capillary centerline. This was due to the heat generated by Joule effect that moves from the central region to the wall by convection, and then is dissipated through the capillary wall by conduction. The temperature increment due to Joule effect increased the average EO velocity and, as a consequence, mass transfer and dispersion of the species. Tang et al. [10] extended the analysis of Joule heating effects on EOF in polydimethylsiloxane microfluidic channels. The EO velocity profile was found to deviate from the classical plug-like shape, to a concave configuration in the hydrodynamically developing region and to a convex pattern in the fully developed region, due to the Joule heating. Also the sample band shape was distorted, broadening its width and reducing its peak.

Perturbations to the EO velocity profile in a homogeneous capillary due to Joule heating effect was also observed by Xuan et al. [9]. They compared experimental and numerical results founding a good agreement in both the inlet and the outlet regions of the capillary, with a slight underestimation of numerical simulations for the time needed to make stable the flow rate when the electrical field was applied. During the first several seconds after the application of the electric field, a quick increase in the liquid temperature was observed.

Horiuchi and Dutta [12] analysed fluid temperature distribution under different conditions. In case of isothermal channel surfaces, when the channel surface temperature was higher than the inlet temperature of fluid, an increase of dimensional fluid temperature was found as the flow progressed. Conversely, in case of channel surface temperature lower than the inlet temperature of fluid, the local fluid temperature and heat flux decreased along the channel. Under constant surface heat flux conditions, the fluid temperature increased monotonically along the channel in case of heat addition to the channel, whereas it decreased in case of heat rejection. However the temperature distribution was observed to remain constant across the channel after ten characteristic dimensions from the entrance. Finally, it was found that the contribution of Joule heating needs to be taken into account only for channels larger than 20 μm.

Nithiarasu and Eng [11] proposed a modelling procedure for studying Joule heating due to EOF. The fluid temperature distribution was found to be different along the channel: a rapid temperature variation was observed in the inlet region, whereas a constant value was detected in the outlet region, where the heat transferred and heat generated are approximately equal.

Sánchez et al. [5] observed that the temperature gradients along the capillary make the electric and flow fields non-uniform along the axial and longitudinal directions due to the dependence of viscosity and electrical conductivity on temperature.

Vocale et al. [8] compared EOF in elliptical and rectangular geometries in order to optimize thermal performance of the micro heat sinks. They demonstrated that rectangular cross-sections are more effective in case of small values of aspect ratio, whereas the elliptical microchannels are preferable as the aspect ratio increases. Misra and Sinha [14] observed a reduction in fluid temperature as the temperature-jump or the vertical distance between channel walls increase. Shit et al. [3] derived a mathematical model to analyse EOF and heat transfer of power-law fluids in a hydrophobic micro-channel by considering a constant heat source at the boundary of the channel.

Due to the small scale of the phenomenon, the collection of experimental data is quite difficult, especially in complex geometries, such as channels packed with solid particles. Hence numerical modelling is very used to study EOF, but many simplifying assumptions are considered [15] For this reason, the authors analyse EOF in a channel packed with charged solid particles, with prescribed geometric characteristics, using a microscopic approach, that provides minute details of the quantities of interest [16]. To the authors' knowledge, the effect of introducing solid particles on heat transfer due to EO is here investigated for the first time. For this reason, a comparative study between micro-channels

with and without solid charged obstructions is presented. Since EO is commonly used for cooling applications and recently porous media have been introduced to enhance fluid flow, understanding heat transfer phenomena due to EOF through flow obstructions is fundamental.
The aim of the work is to analyse fluid flow and heat transfer due to electro-osmosis and to estimate the effect of introducing charged solid particles. The numerical model proposed and boundary conditions used in this study are presented in Section 2: it is composed of two sets of equations, one to study the electrical field, and the other, based on Navier Stokes equations, for fluid flow and heat transfer. The finite element method is used to discretize the sets of equations and the Characteristic Based Split (CBS) algorithm [17, 16] is used to solve the Navier Stokes equations. In order to highlight the influence of charged solid particles inside the channel, a comparative study between micro-channels with and without solid particles is presented in Section 3. Finally, some conclusions are drawn in Section 4.

Nomenclature

A	Area (m^2)
e	Electron charge (C)
E	External electric field (V/m)
J	Non dimensional parameter in source term of momentum equation
Jo	Non dimensional parameter in source term of energy equation
k	Thermal conductivity ($JK^{-1}m^{-1}$)
k_B	Boltzmann's constant (JK^{-1})
L	Length (m)
n_0	Ionic number concentration in the bulk solution (m^{-3})
p	pressure (Pa)
Pr	Prandtl number
Re	Reynolds number
T	Temperature (K)
$\mathbf{u}$	Velocity vector (m/s)
W	Width (m)
z	Valence of the ions
Greek symbols	
β	Artificial compressibility parameter
ϵ	Dielectric constant of the electrolyte
ϵ_0	Permittivity of the vacuum ($Cm^{-1}V^{-1}$)
ζ	Zeta potential (V)
κ	Debye length (m^{-1})
μ_f	Viscosity of the bulk solution (Nsm^{-2})
ϕ	Applied voltage (V)
ρ	Density (kgm^{-3})
ρ_e	Net charge density in the fluid (Cm^{-3})
σ	Electrical conductivity (Sm^{-1})
ψ	Electric potential inside the fluid (V)
Subscripts	
ref	Reference
f	Fluid

2. Mathematical model and solution procedure

The aim of this work is to numerically model Electro-Osmotic Flow (EOF), heat transfer and Joule heating in micro-channels filled with an electrolyte, with and without solid charged particles. The numerical model used for the simulations is based on two sets of equations, one to analyse the electro-kinetic effects, the other for fluid flow and heat transfer. External electric field, ϕ, and internal potential, ψ, are determined by solving the Laplace and Poisson-Boltzmann equations, respectively. Both the equations are shown in their non-dimensional form:

- *Laplace equation*

$$\sigma^* \nabla^2 \phi^* = 0 \tag{1}$$

- *Poisson-Boltzmann equation*

$$\nabla^2 \psi^* = -\left(\kappa L_{ref}\right)^2 \sinh\left(\psi^*\right) \tag{2}$$

where σ^* is the non dimensional electrical conductivity, κ, known as Debye-Hückel parameter, is the reciprocate of the EDL thickness [18], defined as:

$$\kappa = \left(\frac{2n_0 z^2 e^2}{k_B T_{ref} \epsilon \epsilon_0}\right)^{1/2} \tag{3}$$

in which n_0 is the ionic number concentration in the bulk solution, z is the valance of the ions, e is the elementary charge, k_B is the Boltzmanns constant, T_{ref} is the reference temperature measured in kelvin, ϵ is the dielectric constant of the electrolyte, ϵ_0 is the permittivity of vacuum. L_{ref} is an equivalent reference length introduced to take into account the effect of the charge of solid particles on EOF and defined as [15]:

$$L_{ref} = \frac{A_f}{L} \tag{4}$$

in which A_f is the area of the channel occupied by the fluid, and L is the length of the channel. In plain channels, L_{ref} corresponds to the channel width, consistent with the quantity commonly used in previous works concerning EOF, while in channels with flow obstructions, its use allows to take into account flow enhancement due to the charge of solid particles. The dimensionless form for forced flow can be obtained through the following non-dimensional scales.

$$x_i^* = \frac{x_i}{L_{ref}}; \quad \phi^* = \frac{\phi}{\phi_{max}}; \quad \psi^* = \frac{ze\psi}{k_B T}; \quad \rho^* = \frac{\rho_f}{\rho_{ref}}; \quad u_i^* = \frac{u_i}{u_{ref}}; \quad u_{ref} = \frac{E\epsilon\epsilon_0\zeta}{\mu_f}; \quad p^* = \frac{p - p_{ref}}{\rho_{ref} u_{ref}^2}$$

$$t^* = \frac{t u_{ref}}{L_{ref}}; \quad T^* = (T - T_{ref})\frac{2k}{\sigma\phi_{max}^2}; \quad \sigma^* = \frac{\sigma_f}{\sigma_{ref}}; \quad Re = \frac{\rho_{ref} u_{ref} L_{ref}}{\mu_{ref}}; \quad J = \frac{2n_0 ze\phi_{max}}{u_{ref}^2 \rho_{ref}}; \quad Jo = \frac{1}{RePr}$$

The effect of the equations governing the electro-kinetic effects is introduced into the Navier-Stokes equations [18] to simulate fluid flow and heat transfer due to electro-osmosis, through a source term in the momentum and the energy equations. The non-dimensional Navier-Stokes equations modified to take into account the electro-kinetic effects are written as:

- *Continuity equation*

$$\nabla \cdot \mathbf{u}^* = 0 \tag{5}$$

- *Momentum equation*

$$\frac{\partial \mathbf{u}^*}{\partial t^*} + \mathbf{u}^* \cdot \nabla \mathbf{u}^* = -\nabla p^* + \frac{1}{Re}\nabla^2 \mathbf{u} + J \sinh(\psi^*)\left(-\frac{\partial \phi^*}{\partial x_i^*}\right) \tag{6}$$

- *Energy equation*

$$\frac{\partial T^*}{\partial t^*} + \mathbf{u}^* \cdot \nabla T^* = \frac{k^*}{RePr} + \sigma^* Jo\left(-\frac{\partial \phi^*}{\partial x_i^*}\right)^2 \tag{7}$$

where Re is the Reynolds number, Pr is the Prandtl number, J and Jo are the non dimensional coefficients for the source terms of momentum and energy equation, respectively, and k is the thermal conductivity.
The equations are solved using the finite element method combined with the Characteristic-Based Split (CBS) algorithm [17].
With reference to Fig. 1, the walls of the channel and any solid boundary are assumed to be active with a prescribed non-dimensional zeta potential and to obey no-slip velocity boundary conditions. Channel walls and inlet temperature are assumed to be constant and equal to the reference temperature, whereas the boundaries of solid particles are assumed to be adiabatic. An applied external potential difference between inlet and outlet is considered and the normal velocity gradients are assumed to be zero at both inlet and outlet.

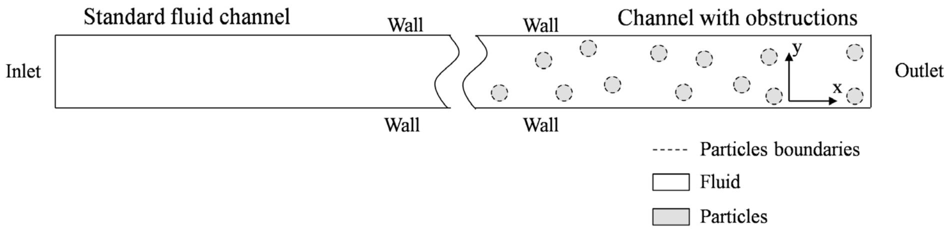

Fig. 1. Boundary conditions.

3. Results and discussion

A two-dimensional rectangular channel, 60 μm in width and characterised by an aspect ratio equal to 10, is considered for the simulations. A plain channel and a channel filled with regular circular obstructions are analysed. The obstructions are characterized by a diameter equal to 16% of channel width. An electrical field equal to 1 kV/m is applied and deionized water is used as working fluid. The other parameters used in the present study are reported in Table 1. A set of 2D unstructured meshes, refined near all solid boundaries to capture the higher gradients of both

Table 1. Parameters used in the numerical simulations.

Parameter	Measurement unit	Value
Zeta potential, ζ	-19.2	V
Dielectric constant of the electrolyte, ϵ	78.4	-
Ionic concentration in the bulk solution, n_0	$6.02 \cdot 10^{+19}$	m^{-3}
Valence of the ions, z	1	-
Reference temperature, T_{ref}	298	K
Fluid density, ρ_f	1000	kg/m^3
Fluid viscosity, μ_f	$8.91 \cdot 10^{-4}$	$Pa \cdot s$
Electrical conductivity, σ_{ref}	0.20	$S \cdot m^{-1}$

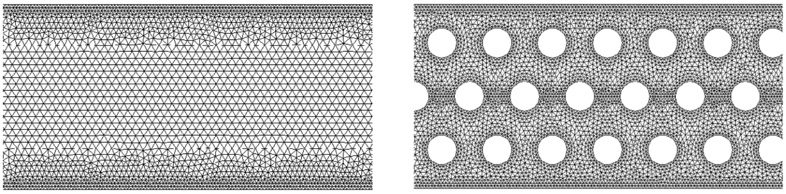

Fig. 2. Details of the meshes used for fluid and channel with obstructions.

internal potential and velocity, are used. The details of the meshes used for plain channels and channels with obstructions are shown in Fig. 2. A mesh sensitivity study has been carried out to optimise the elements number used in the calculations. In Fig. 3, the internal potential and horizontal velocity distribution for plain channel and channel packed with charged solid particles are shown; only a detail is presented for the sake of clearness. The presence of charged solid particles enhances the internal potential distribution, making its value different from zero in a larger fraction of the channel with respect to the case of plain channel, as illustrated in Fig.s 3a and 3b. Since the internal potential appears in the source term of momentum equation, it positively influences also the velocity field, as highlighted in Figure 3c and 3d. The local value of horizontal velocity is significantly affected by the charge of solid particles. De-

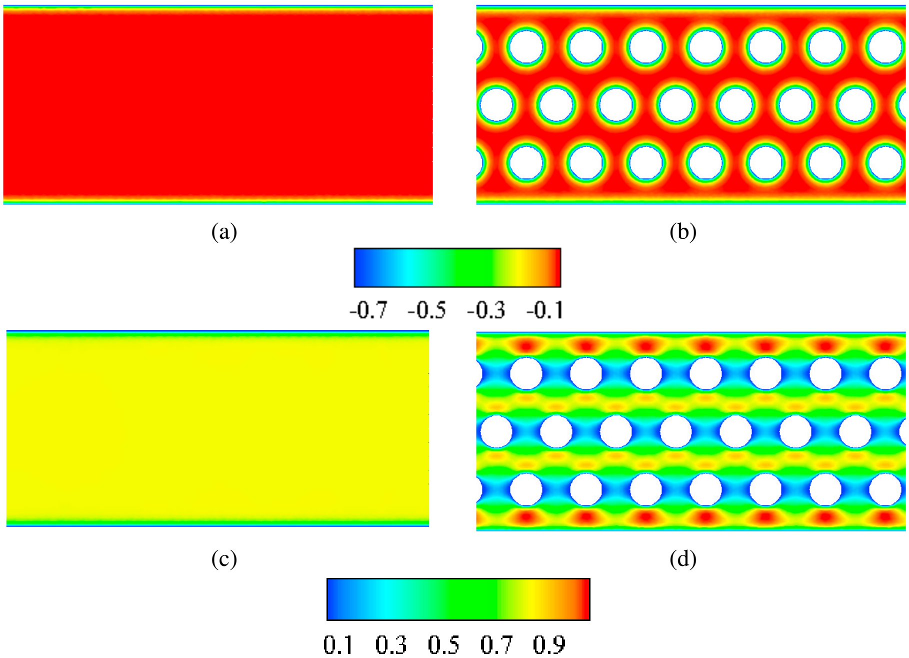

Fig. 3. Internal potential and horizontal velocity distribution in plain channel (a-c) and channel packed with charged solid particles (b-d).

spite this, the outlet average velocity, and therefore flow rate that can be produced, is higher in plain channels. This is due to the resistant effect opposed by the particles to fluid flow. As shown in Fig. 4, electro-osmosis plays a role on heat transfer: temperature increases as the distance from the channel wall and the inlet section, that are at ambient temperature, increases. Introducing charged adiabatic solid particles in the channel affects temperature distribution, involving a lower increase due to electro-osmosis. This aspect needs to be better investigated since it can be attractive in electro-osmotically flow driven systems aimed at cooling micro-devices. It is worth noticing that for both configurations, temperature increase is confined to the central region of the channel.

For the sake of clarity, the profiles in the vertical direction of internal potential, velocity and temperature distributions are shown in Fig.s 5 and 6. These profiles are constant along the channel in case of plain channels, whereas they change when solid obstructions are introduced. In order to assess the effect of charged solid particles, in this case the

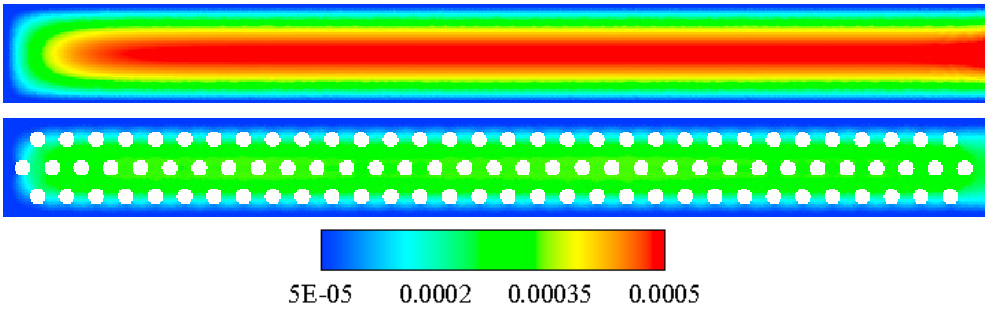

Fig. 4. Temperature distribution in plain channel and channel packed with charged solid particles.

profiles are shown at different sections of the channels. As previously shown, the internal potential is not equal to zero in a larger section of the channel when obstructions are introduced and its gradient is steeper close the charged surface of the particle. As shown in Fig. 6a, the horizontal velocity is significantly influenced by the internal potential:

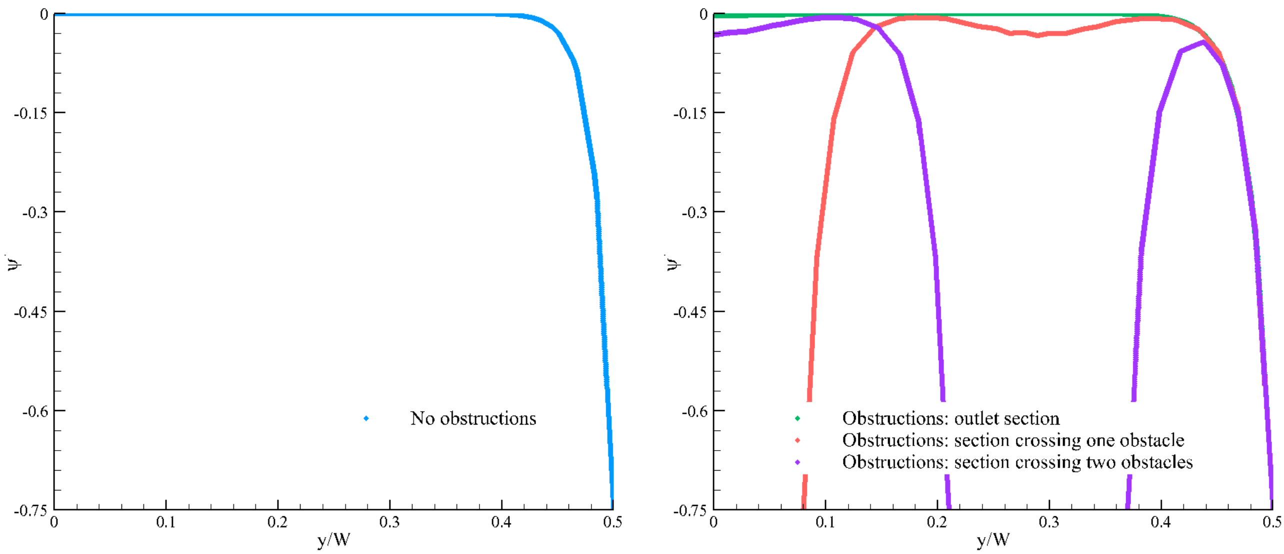

(a) (b)

Fig. 5. Internal potential profile in plain channel (a) and channel packed with charged solid particles at different sections (b).

the maximum values are obtained in correspondence of the highest gradients of the internal potential. Temperature shows a parabolic profile, whose magnitude is greater for the plain channel. In the channel with solid obstructions, the temperature is higher in sections crossing the particles.

4. Conclusions

Electro-osmotic flow through micro-channels with and without charged solid particles has been investigated. The introduction of solid particles enhances internal potential within the channel and, as a consequence, affects velocity distribution. Also temperature distribution is slightly influenced by the presence of solid particles. This aspect should be focused by investigating different operating conditions and micro-channel sizes, since temperature increase plays a fundamental role in some fields of application of electro-osmotically flow driven systems, such as cooling o micro-devices.

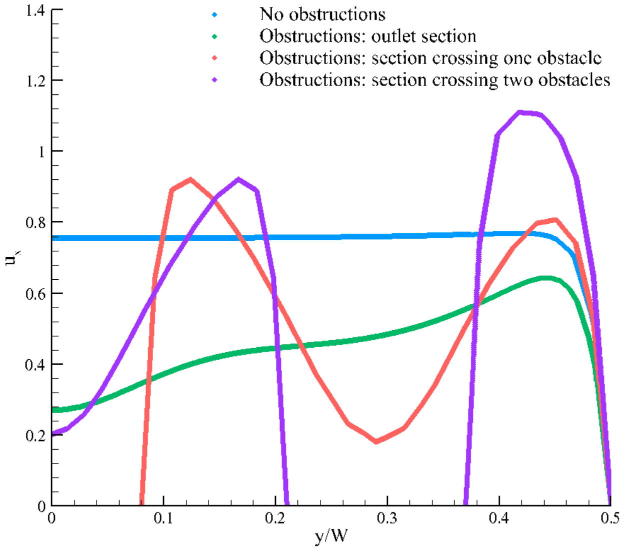

(a)

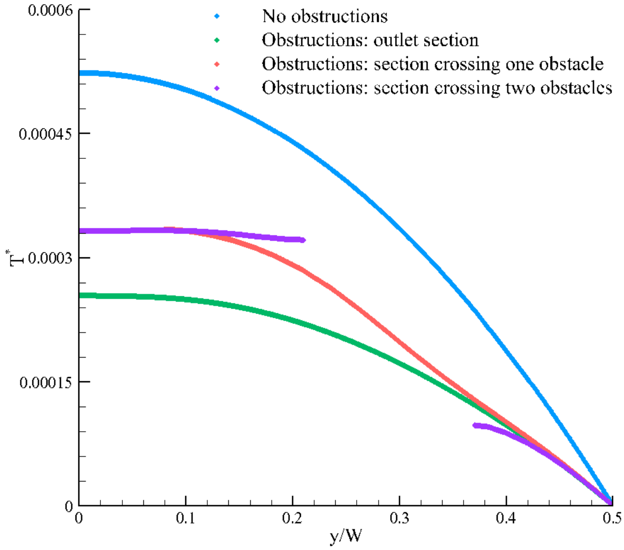

(b)

Fig. 6. Horizontal velocity (a) and temperature (b) profiles.

References

[1] Ronghui Qi, Changqing Tian, and Shuangquan Shao. Experimental investigation on possibility of electro-osmotic regeneration for solid desiccant. *Applied Energy*, 87(7):2266–2272, 2010.

[2] P Nithiarasu and RW Lewis. A short note on joule heating in electro-osmotic flows: A consistent non-dimensional scaling. *International Journal of Numerical Methods for Heat & Fluid Flow*, 18(7/8):919–931, 2008.

[3] GC Shit, A Mondal, A Sinha, and PK Kundu. Electro-osmotic flow of power-law fluid and heat transfer in a micro-channel with effects of Joule heating and thermal radiation. *Physica A: Statistical Mechanics and its Applications*, 462:1040–1057, 2016.

[4] Ronald F Probstein. *Physicochemical hydrodynamics: an introduction*. John Wiley & Sons, 2005.

[5] S Sanchez, F Mendez, L Martinez-Suastegui, and O Bautista. Asymptotic analysis for the conjugate heat transfer problem in an electro-osmotic flow with temperature-dependent properties in a capillary. *International Journal of Heat and Mass Transfer*, 55(25):8163–8171, 2012.

[6] JC Misra and S Chandra. Electro-osmotic flow of a second-grade fluid in a porous microchannel subject to an ac electric field. *Journal of Hydrodynamics, Ser. B*, 25(2):309–316, 2013.

[7] GY Tang, Chun Yang, JC Chai, and HQ Gong. Joule heating effect on electroosmotic flow and mass species transport in a microcapillary. *International Journal of Heat and Mass Transfer*, 47(2):215–227, 2004.

[8] P Vocale, M Geri, L Cattani, GL Morini, and M Spiga. Electro-osmotic heat transfer in elliptical microchannels under H1 boundary condition. *International Journal of Thermal Sciences*, 72:92–101, 2013.

[9] Xiangchun Xuan, Bo Xu, David Sinton, and Dongqing Li. Electroosmotic flow with Joule heating effects. *Lab on a Chip*, 4(3):230–236, 2004.

[10] Gongyue Tang, Deguang Yan, Chun Yang, Haiqing Gong, John Chee Chai, and Yee Cheong Lam. Assessment of Joule heating and its effects on electroosmotic flow and electrophoretic transport of solutes in microfluidic channels. *Electrophoresis*, 27(3):628–639, 2006.

[11] P Nithiarasu, PF Eng, et al. Numerical modelling of heat generated by electroosmotic flows in micro-channels. 2009.

[12] Keisuke Horiuchi and Prashanta Dutta. Joule heating effects in electroosmotically driven microchannel flows. *International journal of heat and mass transfer*, 47(14):3085–3095, 2004.

[13] Yong Shi, TS Zhao, and Zhaoli Guo. Simplified model and lattice boltzmann algorithm for microscale electro-osmotic flows and heat transfer. *International journal of heat and mass transfer*, 51(3):586–596, 2008.

[14] J.C. Misra and A. Sinha. Electro-osmotic flow and heat transfer of a non-Newtonian fluid in a hydrophobic microchannel with navier slip. *Journal of Hydrodynamics, Ser. B*, 27(5):647 – 657, 2015.

[15] S Di Fraia, N Massarotti, and P Nithiarasu. Effectiveness of flow obstructions in enhancing electro-osmotic flow. *Microfluidics and Nanofluidics*, 21(3):46, 2017.

[16] F Arpino, G Cortellessa, and A Mauro. Transient thermal analysis of natural convection in porous and partially porous cavities. *Numerical Heat Transfer, Part A: Applications*, 67(6):605–631, 2015.

[17] P Nithiarasu. An efficient artificial compressibility (AC) scheme based on the characteristic based split (CBS) method for incompressible flows. *International Journal for Numerical Methods in Engineering*, 56(13):1815–1845, 2003.

[18] Neelesh A Patankar and Howard H Hu. Numerical simulation of electroosmotic flow. *Analytical Chemistry*, 70(9):1870–1881, 1998.